FED-Vol. 236, 1996 Fluids Engineering Division Conference
Volume 1
ASME 1996

AIR-WATER BUBBLY FLOW IN FREE-SHEAR LAYERS

H. CHANSON
Department of Civil Engineering
The University of Queensland
Brisbane QLD 4072
Australia

T. BRATTBERG
Department of Civil Engineering
The University of Queensland
Brisbane QLD 4072
Australia

INTRODUCTION

Air-water bubbly flows are encountered in many engineering applications ranging from chemical engineering to mechanical engineering applications (e.g. WOOD 1991, CHANSON 1995). In some cases, free-surface aeration is maximised (e.g. for re-oxygenation). In others, it must be minimised or prevented (e.g. with fire-fighting equipment and Pelton turbine jets). In some flow situations, flow aeration is not controlled (e.g. along a spillway). In each case, however, the knowledge of the air bubble/turbulence interactions is very important to predict accurately the air-water flow properties, hence to optimise the system performances and to insure a safe operation.

One type of air-water shear flows is the developing flow region of a plunging jet (fig. 1 and 2). In chemical engineering, plunging jets are used to stir chemicals as well as to increase gas-liquid transfer (e.g. McKEOGH and ERVINE 1981, BIN 1993). In sewage and water treatment plants, aeration cascades combine the effects of flow aeration and high turbulence level, enhancing the mass transfer of volatile gases (e.g. oxygen, nitrogen, volatile organic compounds). Despite the wide range of applications few studies investigated air bubble entrainment in the developing shear layer of plunging jets, at the exception of BONETTO and LAHEY (1993), CUMMINGS (1995) and the first author (CHANSON 1995).

In the present paper, new experiments performed with a vertical two-dimensional plunging jet are described. The study focused on the air-water flow properties in the developing shear layer. Distributions of air concentration and mean velocity are presented. The results are compared with an analytical solution of the air bubble diffusion equation. Distributions of bubble chord length are also shown.

EXPERIMENTAL INVESTIGATIONS

Experimental apparatus

Experimental investigations were conducted in the two-dimensional supported plunging jet experiment of the University of Queensland (fig. 1). The apparatus consists of a glass tank (1.8-m deep, 0.30-m wide, 3.6-m long) and a vertical nozzle supplying a planar supported jet (0.269-m wide, 0.012-m jet thickness at nozzle). The length of the jet support is 0.35 m. The water supply comes from a constant head tank with a constant water level of 12.9 m above the nozzle. Domestic water was used in all experiments.

Instrumentation.

Clear-water velocities were measured using a Pitot tube (external diameter Ø = 3.3 mm). The Pitot tube was connected either to a Validyne™ DP15 pressure transducer scanned at 500 Hz or to a vertical manometer used to calibrate the transducer. Identical results were obtained in both cases.

Single-tip and double-tip conductivity probes were used during the experiments. Air concentration measurements were usually performed with the single-tip conductivity probe. The probe consists of a sharpened rod (platinum wire Ø = 0.35 mm) which is insulated except for its tip and set into a metal supporting tube (stainless steel surgical needle Ø = 1.42 mm) acting as the second electrode. A two-tip conductivity probe was used to record the air-water velocity based upon a cross-correlation technique between the signals of the two tips aligned in the direction of the flow. The probe could be used also for air concentration measurements. The combination of the cross-correlation result and the signal at the leading tip enabled the estimate of bubble chord length distributions. Each tip is identical (internal diameter of 25 µm, external diameter of 200 µm) and they are spaced 8-mm apart.

The conductivity probes were excited by an air bubble detector (AS25240) connected to a high-speed data acquisition system. Most measurements were recorded with a scanning rate of 40 kHz per channel.

Further, additional information was obtained by visual observations using high-speed photographs (flash speed of 33 µs) (e.g. fig. 3).

Full details of the experimental apparatus and instrumentation, and experimental results of CHANSON (1995) and CUMMINGS (1995) were reported in CHANSON (1995).

Table 1- Experimental flow conditions (2-D supported jet, θ = 89 degrees, W = 0.269 m)

Ref.	Run	q_w	V_1	x_1 [a]	d_1	Comments
		m^2/s	m/s	m	m	
(1)	(2)	(3)	(4)	(5)	(6)	(6)
University of Queensland						
CHANSON (1995)	F1	0.024	2.36	0.090	0.0102	Tu=1.70 %.
	F2	0.048	4.06	0.090	0.0118	Tu=1.50 %.
	F3	0.072	5.89	0.090	0.0122	Tu=0.74 %.
	F4	0.096	8.0	0.090	0.012	
	F5	0.108	9.0	0.090	0.012	
CUMMINGS (1995)	2-m/s	0.0235	2.35	0.0875	0.010	Tu=1.6 %.
	6-m/s	0.072	6.14	0.0875	0.0117	Tu=0.75 %.
New results	3-m/s	0.032	3.0	0.10	0.0106	Tu=1.25 %.

Notes :
([a]) : longitudinal distance between the nozzle and the free-surface pool; W : channel width; θ : jet angle with the horizontal; q_w : plunging jet flow rate per unit width; Tu : jet turbulence intensity at impact (measured outside of the support boundary layer).

Experimental results

During the experiments (table 1), the free-surface of the receiving pool of water was located at about 0.1 m below the jet nozzle. At the jet impact with the free-surface, the flow conditions were partially-developed : i.e., the relative boundary layer thickness δ_{99}/d_1 was less than 0.2.

The new series of measurements included air concentration and velocity distributions below the entrainment point as well as measurements of air bubble chord lengths. Results are reported on figures 4 and 5 at various locations below the impingement point.

AIR BUBBLE DIFFUSION

In the air bubble diffusion layer of a plunging jet, the basic equation of air bubble diffusion can solved for both two-dimensional jets and circular jets (CHANSON 1995). For a bi-dimensional jet, the solution of the diffusion equation is :

$$C = \frac{q_{air}}{V_1 * \sqrt{4 * \pi * \frac{D_t}{V_1} * (x - x_1)}} * \exp\left(- \frac{V_1}{4 * D_t} * \frac{(y - Y_{Cmax})^2}{x - x_1} \right) \quad (1)$$

where C is the void fraction (or air concentration), q_{air} is the volume air flow rate per unit width, V_1 is the impact flow velocity ($V_1 = q_w/d_1$), d_1 is the supported-jet thickness at impact, x is the distance in the flow direction (fig. 1), x_1 is the distance between the nozzle and the impingement point, y is measured normal to the flow direction (fig. 1), Y_{Cmax} is the location where the air content is maximal and D_t is the turbulent diffusivity. Experimental results are compared with equation (1) on figure 4.

Note that, for advective diffusion of matter in monophase flow and uniform velocity distribution, $Y_{Cmax} = d_1$.

Momentum shear layer

In the developing flow region, the motion equation can be analysed as a free-shear layer. For a plane shear layer GOERTLER (1942) solved the equation of motion assuming a constant eddy viscosity ν_T across the shear layer :

$$\nu_T = \frac{1}{4 * K^2} * (x - x_1) * V_1 \quad (2)$$

where K is a constant. GOERTLER (1942) obtained the solution in the first approximation :

$$\frac{V}{V_1} = \frac{1}{2} * \left(1 + \text{erf}\left(\frac{K * (y - y_{50})}{x - x_1} \right) \right) \quad (3)$$

where V is the velocity, y_{50} is the location where $V = V_1/2$ and the function erf is defined as :

$$\text{erf}(u) = \frac{2}{\sqrt{\pi}} * \int_0^u \exp(-t^2) * dt \quad (4)$$

Equation (3) compares 'reasonably well' with experimental data. A dominant feature is that the momentum shear layer does NOT coincide with the air bubble diffusion layer. With vertical supported plunging jets, it is observed consistently that $y_{50} > Y_{Cmax} > d_1$ (e.g. fig. 4).

Interactions between advective diffusion and shear layer

The author estimated the turbulent diffusivity D_t satisfying equation (1) for each experiment. The results are reported in table 2.

The results indicate that the ratio D_t/ν_T is about unity (or slightly greater than one), ν_T being the eddy viscosity (table 2). D_t/ν_T compares the effects of both : 1- the difference in the diffusion of a discrete air bubble particle and the diffusion of a small coherent fluid structure, and 2- the influence of the air bubble on the turbulence field. The relatively-large values of D_t/ν_T suggest that the air bubble diffusion mechanism is not strongly affected by the shear layer flow.

Table 2 - Turbulent diffusivity for the experiments

Ref.	Run	V_1	D_t	ν_T	$\frac{D_t}{V_1 * d_1}$	$\frac{D_t}{\nu_T}$
		m/s	m^2/s	m^2/s		
(1)	(2)	(3)	(4)	(5)	(6)	(7)
CHANSON	F1	2.36	9.4E-4		3.9E-2	
(1995)	F2	4.06	8.8E-4		1.8E-2	
	F3	5.89	2.7E-3		3.7E-2	
	F4	8.00	5.85E-3		6.1E-2	
	F5	9.00	5.7E-3		5.3E-2	
CUMMINGS (1995)	2-m/s	2.35	9.4E-4 ([a])	2.62E-4 ([b])		3.2
	6-m/s	6.14	2.7E-3 ([a])	1.93E-3 ([b])		1.3
New results	3-m/s	3.0	1.0E-3	2.3E-3 ([b])	3.1E-2	0.43

Notes : ([a]) : estimated by the authors; ([b]) : computed using equation (2) at $(x - x_1) = 0.05$ m

DISCUSSION

Air bubble chord length distributions were recorded with the double-tip conductivity probe. The bubble chord length is defined as the length of the straight line connecting the two intersections of the air-bubble free-surface with the leading tip of the probe as the bubble is transfixed by the probe sharp-edge.

A complete set of results is reported on figure 4 where the normalised probability is plotted as a function of the distance from the vertical support and of the chord length. The data are presented for several chord length bands : 0.1-1 mm, 0.5-10 mm, 2-40 mm. For each figure, the histogram points represent each the probability of a bubble chord length in a chord length interval (0.1-mm, 0.5-mm, 2-mm on fig. 5A, 5B, 5C respectively). E.g., on figure 5A, the probability of bubble chord length from 0.2 to 0.3 mm is represented by the column labelled 0.3-mm. All data (fig. 5) were recorded at 50-mm below the impingement point (i.e. $(x - x_1) = 0.05$ m).

Figure 5 shows that the range of chord length extends over several order of magnitude : i.e., from less than 0.1 mm up to over 50 mm. Further the distributions of bubble chord length are nearly the same across the shear layer flow.

Air entrainment process

At *low jet velocities*, the plunge pool water is unable to follow the undulations of the jet surface. Air enters the flow following the passage of these disturbances through the interface between the jet and the receiving flow (fig. 2A). The entrainment process is intermittent and pulsating. High-speed photographs show the *entrainment of individual elongated air packets* (e.g. fig. 3) (see also CHANSON and CUMMINGS 1994). The air packets can be later broken up into smaller bubbles.

With *high jet velocities* (i.e. $V_1 > 5$ to 10 m/s), the air entrainment process is modified. At the impingement point the flow is unsteady and rapidly-varied. And a thin sheet of air is set into motion by shear forces at the surface of the jet at the impact point (fig. 2B). The *air sheet* behaves as a *ventilated cavity* (e.g. MICHEL 1984) : the length of the air layer fluctuates considerably and air pockets are entrained by *discontinuous 'gusts'* at the lower end of the air layer (fig. 2B). The elongated air sheet is intermittently broken up by a *'re-entrant jet' mechanism*. Visual observations and measurements show clearly that some air is entrained in the form of large elongated pockets ('finger' shape). The entrained air packets are broken up into smaller bubbles in the turbulent shear layer.

Most bubbles are broken up over short distances (i.e. $\Delta x \sim$ 50 to 100 mm). And the time-scale of the breakup process is typically of about 20 milliseconds (for V_1 in the range 2.4 to 6.1 m/s).

CONCLUSION AND SUMMARY

Air bubble entrainment at a vertical supported plunging jet has been investigated experimentally. The study is focused on the developing shear layer below the entrainment point.

The experimental data indicate that the advective diffusion of air bubbles is little affected by the shear flow. The symmetry axis of the air diffusion layer is only slightly shifted outwards. The air-water velocity data indicate that the shape of the velocity distribution is the same as for monophase flow. But the shear layer is shifted away from the support. The momentum shear layer is 'shifted outwards' in comparison with the air bubble diffusion layer. And it is consistently observed that $y_{50} > Y_{Cmax} > d_1$.

Chord length distributions extend over a broad range (i.e. typically from 0.1 to 50 mm). Such a result is confirmed by photographic observations showing elongated air pockets (i.e. 'finger' shape) being entrainment by instabilities and re-entrant jet at the entrainment point.

ACKNOWLEDGEMENTS

The writers thank Mr P.D. CUMMINGS for his helpful comments and Professor C.J. APELT for his support.

The project was sponsored by the Australian Research Council (Ref. No. A89331591). The junior writer acknowledges the Australian Postgraduate Award supported by the Australian Research Council (Ref. No. A8941296).

REFERENCES

BIN, A.K. (1993). "Gas Entrainment by Plunging Liquid Jets." *Chem. Eng. Science*, Vol. 48, No. 21, pp. 3585-3630.

BONETTO, F., and LAHEY, R.T. Jr (1993). "An Experimental Study on Air Carryunder due to a Plunging Liquid Jet." *Intl Jl of Multiphase Flow*, Vol. 19, No. 2, pp. 281-294.

CHANSON, H. (1995). *Report CH46/95*, Dept. of Civil Engineering, Univ. of Queensland, Australia, 368 pages.

CHANSON, H., and CUMMINGS, P.D. (1994). "An Experimental Study on Air Carryunder due to Plunging Liquid Jet - Discussion." *Intl Jl of Multiphase Flow*, Vol. 20, No. 3, pp. 667-770.

CUMMINGS, P.D. (1995). "Air Entrainment by Plane Plunging Jets." *Report CH46/95*, H. CHANSON Editor, Dept. of Civil Engineering, Univ. of Queensland, Australia, pp. 4-1/4-16.

GOERTLER, H. (1942). "Berechnung von Aufgaben der freien Turbulenz auf Grund eines neuen Näherungsansatzes." *Z.A.M.M.*, 22, pp. 244-254 (in German).

McKEOGH, E.J., and ERVINE, D.A. (1981). "Air Entrainment rate and Diffusion Pattern of Plunging Liquid Jets." *Chem. Engrg. Science*, Vol. 36, pp. 1161-1172.

MICHEL, J.M. (1984). "Some Features of Water Flows with Ventilated Cavities." *Jl of Fluids Eng.*, Trans. ASME, Sept., Vol. 106, p.319.

WOOD, I.R. (1991). "Air Entrainment in Free-Surface Flows." *IAHR Hydraulic Structures Design Manual No. 4*, Hydraulic Design Considerations, Balkema Publ., Rotterdam, The Netherlands, 149 pages.

STATEMENT OF ACCURACY AND UNCERTAINTY

The authors estimate the accuracy of the measurement techniques as :

- vertical probe positions {x} : $\Delta x < 2$ mm;
- probe position normal to support {y} : $\Delta y < 0.05$ mm;
- water discharge measurement : $\Delta q_w/q_w < 2\%$.
- air concentration (void fraction) : $\Delta C/C = 2$ % for $5 < C < 95\%$; $\Delta C = 2$ % for $C > 95\%$; $\Delta C = 5$ % for $C < 5\%$;
- clear-water velocity : $\Delta V/V = 1$ %;
- mean air-water velocity : $\Delta V/V = 5$ % for $5\% < C < 95\%$; $\Delta V/V = 10$ % for $1\% < C < 5\%$; $\Delta V/V > 20$ % for $C < 1\%$;
- minimum detectable bubble chord length : 50 μm in a 2-m/s flow, 150 μm in a 6-m/s jet;

The entrainment process is by nature a fluctuating process. As a result the higher uncertainties on the data were observed next to the entrainment point :

- air concentration (void fraction) : $\Delta C < 5$ % at $(x\text{-}x_1) = 20$, 30 mm and $\Delta C < 3$ % at $(x\text{-}x_1) = 40$, 50 mm for $5 < C < 95\%$;
- mean air-water velocity : $\Delta V/V = 10$ % at $(x\text{-}x_1) = 20$, 30 mm and $\Delta V/V = 5$ % at $(x\text{-}x_1) = 40$, 50 mm for $5 < C < 95\%$;

Uncertainties are reported on figure 4.

Fig. 1 - Sketch of the vertical supported plunging jet experiment

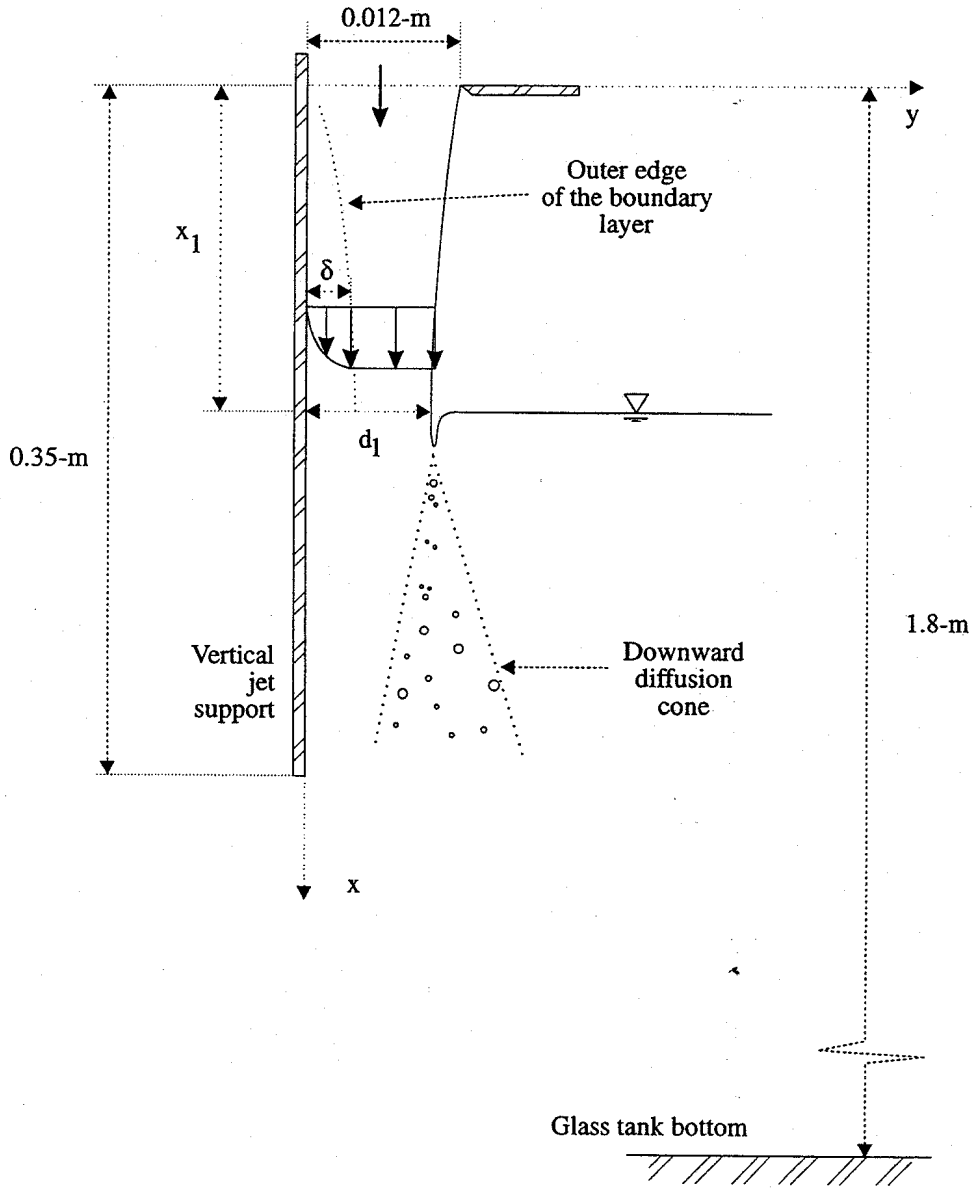

Fig. 2 - Air entrainment at a vertical supported plunging jet
(A) - Mechanisms of air entrainment by low-velocity plunging jets

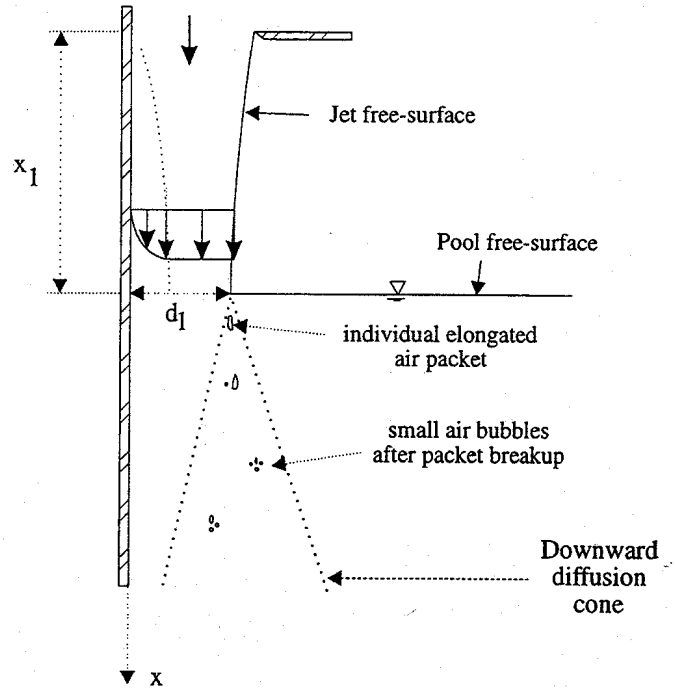

Individual air packet entrainment

(B) Air entrainment by high-velocity plunging jets

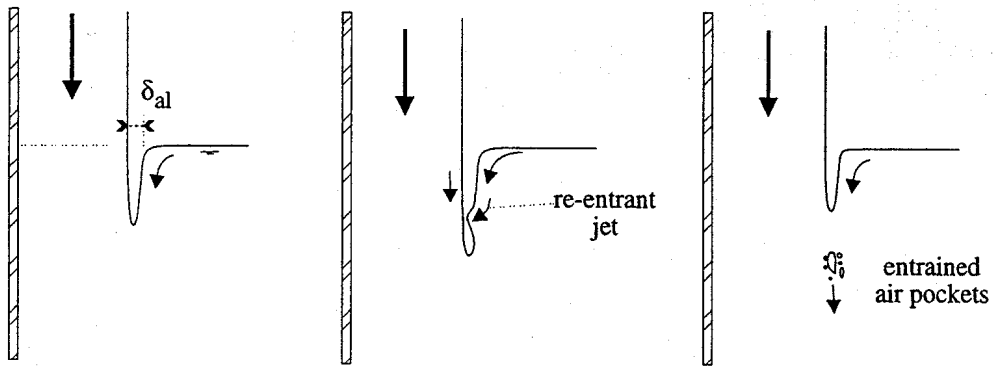

Sequence of large air pocket entrainment

Fig. 3 - Air bubble entrainment at a supported plunging jet
The support of the jet is on the left - $q_w = 0.013$ m^2/s, $x_1 = 0.2$ m, $V_1 = 2.2$ m/s, $d_1 = 0.006$ m
Left : (A) Individual air bubble entrainment : on the right, note the rising air bubbles
Right : (B) Individual air bubble entrainment with intermittent entrainment of large air pockets. Note the elongated air pocket nearly-entrained near the free-surface

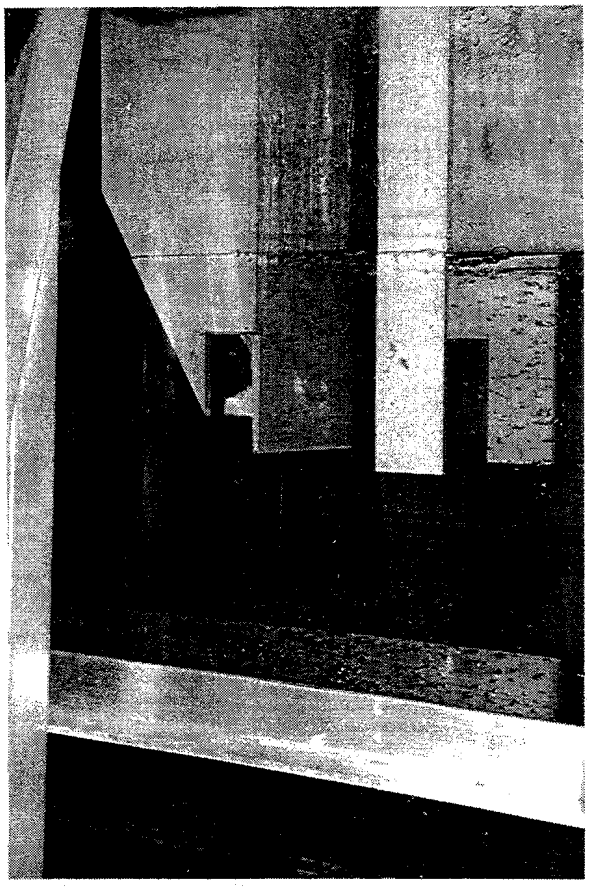

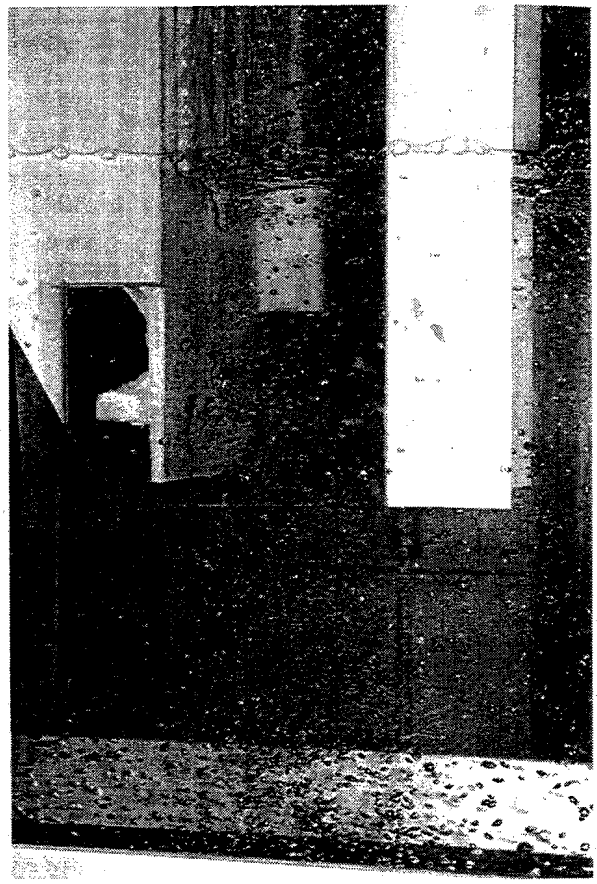

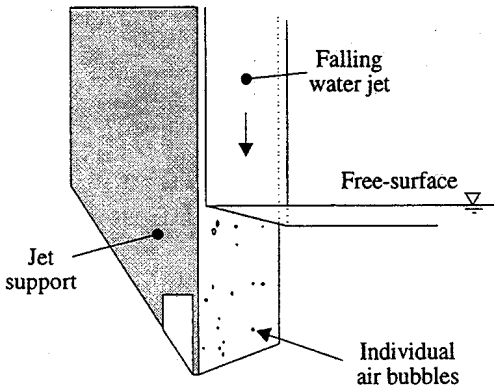

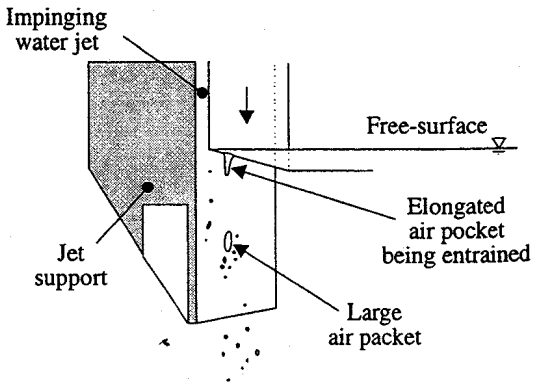

Fig. 4 - Air concentration distributions in the developing shear layer of a vertical supported jet
V_1 = 3.0 m/s, d_1 = 0.011 m, x_1 = 0.1 m.
Comparison between experimental data and analytical solutions

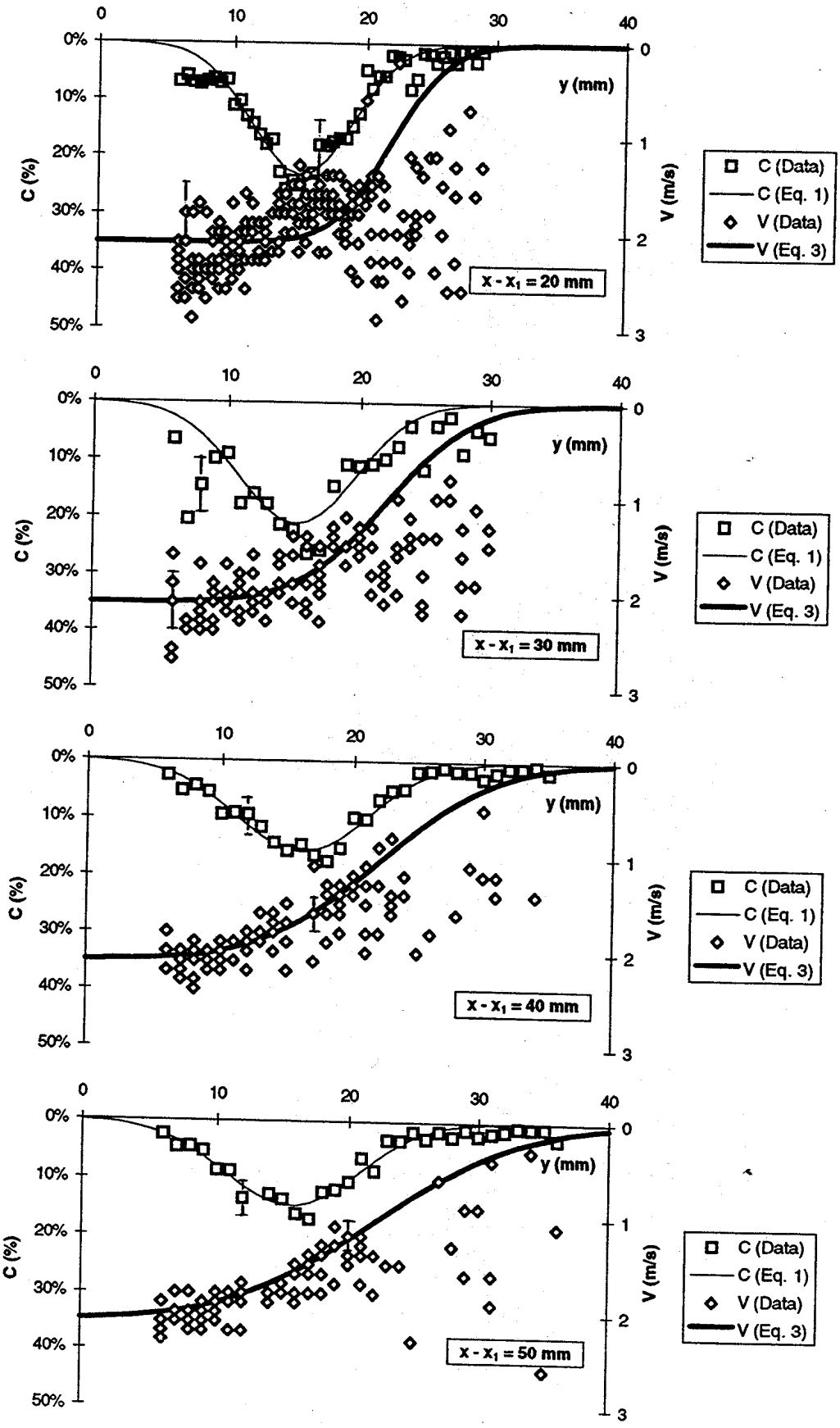

Fig. 5 - Chord length distributions in the air-water shear layer
V_1 = 3.0 m/s, d_1 = 0.011 m, x_1 = 0.1 m, data at x-x_1 = 50 mm.